ACS APPLIED MATERIALS & INTERFACES

Research Article

Cite This: ACS Appl. Mater. Interfaces XXXX, XXX, XXX−XXX

www.acsami.org

Self-Rechargeable-Battery-Driven Device for Simultaneous Electrochromic Windows, ROS Biosensing, and Energy Storage

Yanling Zhai,*,† Ying Li,† Hui Zhang,‡,§ Dengbin Yu,‡,§ Zhijun Zhu,*,† Jinzi Sun,† and Shaojun Dong*,‡,§,∥

†Department of Chemistry and Chemical Engineering, Qingdao University, 308 Ningxia Road, Qingdao, Shandong 266071, China

‡State Key Laboratory of Electroanalytical Chemistry, Changchun Institute of Applied Chemistry, Chinese Academy of Sciences, Changchun, Jilin 130022, China

§University of Science and Technology of China, Hefei, Anhui 230026, China

∥University of Chinese Academy of Sciences, Beijing 100039, China

Supporting Information

ABSTRACT: A self-powered electrochromic device (ECD) powered by a self-rechargeable battery is easily fabricated to achieve electrochromic window design, quantitative reactive oxygen species (ROS) sensing, and energy storage. The special design of the battery was composed of Prussian blue (PB) and magnesium metal as the cathode and anode, respectively, which exhibits fast self-charging and high power-density output for continuous and stable energy supply. Benefitting from the fast electrochromic response of PB, it was not only used for structuring self-rechargeable batteries but also used as an electrochromic display for highly sensitive self-powered ROS sensing and visual analysis. We believe that this work provides a solution to self-powered ECDs limited to a single application and could combine the applications in smart windows, ROS sensing, and other fields together, and in the meantime provide a solution for energy supply problems.

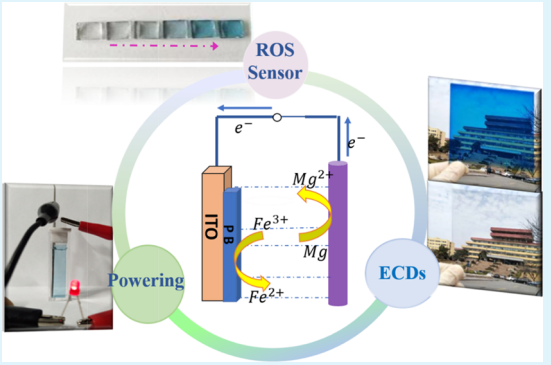

KEYWORDS: *self-powered, electrochromic window, self-rechargeable, ROS biosensor, energy storage*

INTRODUCTION

Electrochromism is a process by which the absorptance, transmittance, emittance, and reflectance of a material can be modulated during chemical reduction/oxidation or charge insertion/extraction.[1−3] Nanomaterials with outstanding electrochromic properties have drawn tremendous scientific interests owing to their low power consumption and high coloration efficiency.[4−6] The most used electrochromic materials are mainly the organic polymers, polyoxometalates, tungsten oxides, Prussian blue (PB), and so on.[7,8] For example, we developed organic−inorganic electrochromic hybrids with excellent electroswitchable properties in aqueous solutions for the first time.[9] So far, various electrochromic devices (ECDs) based on electrochromic materials have been developed for the potential applications in smart windows, information processing, electrical energy storage, and so on.[10] Utilizing polyoxometalate as electrochromic materials, ECDs with multicolored fluorescent switches were reported by Liu's group by assembling CdSe QDs and POMs layer by layer.[11] Later, we developed three-state luminescent ECDs triggered by light, electricity, and chemical inputs for smart window fabrication.[12] However, most of these ECDs are insufficient for multifunctional uses. To address this critical issue, ECDs integrating the electrochromism and other functions, such as energy storage and biosensors, in a smart device should be designed for widespread applications.

However, the operation of conventional ECDs is usually powered by an external stimulus, resulting in additional energy consumption.[11] Although numerous self-powered ECDs driven by nanogenerators,[13] solar cells,[14,15] biofuel cells,[16] and incident light[17] have been recently realized, these devices are much complicated for practical fabrication and operation and especially most of their energy source exhibit low power density output and poor sustainability.[18] To solve this problem, Gibbs-free-energy-supplied ECDs might be an alternative. It is well-known that if high Gibbs free-energy difference exists between anodic and anodic materials, once short circuiting the two electrodes, electron transfer can take place easily and give rise to high power-density output, which presents battery-like characteristics.[19] It is noteworthy that ECDs have been proven to present battery characteristics based on their electrons and ions stored/released during electroswitching.[20] Recently, Wang et al. first reported a bifunctional device combining self-rechargeable battery and

Received: May 20, 2019
Accepted: July 16, 2019
Published: July 16, 2019

Downloaded via BUFFALO STATE on August 1, 2019 at 14:14:17 (UTC).
See https://pubs.acs.org/sharingguidelines for options on how to legitimately share published articles.

© XXXX American Chemical Society

DOI: 10.1021/acsami.9b08715
ACS Appl. Mater. Interfaces XXXX, XXX, XXX−XXX

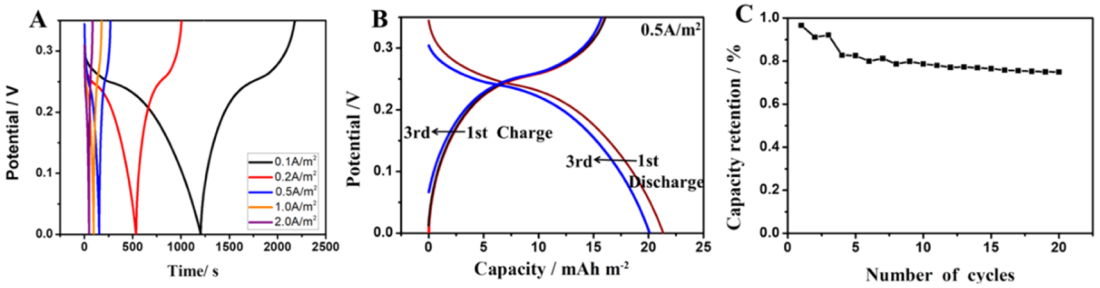

Figure 1. (A) Charge−discharge curves of the PB and Mg battery at a current density of 0.1, 0.2, 0.5, 1.0, and 2.0 A m^{-2}, respectively; (B) the first three galvanostatic charge/discharge cycles of the battery at a current density of 0.5 A m^{-2}, and (C) the cycling performance of the self-powered battery. The PB films are electrodeposited under a constant potential of 0.4 V for 200 s.

self-powered ECDs. Just by connecting the two electrodes can achieve the fast bleaching of the device, then recover to its coloration state oxidized by oxygen in air.[20] Furthermore, they assembled PPy film and Al sheet into another bifunctional self-powered ECD.[21] However, the colored rate of the reported devices was not so fast, which is limited by the weak oxidation of oxygen in air. In this regard, adding a trace amount of NaClO in the electrolyte realized high power density and fast self-charging of the device.[19]

Herein, a prototype of a self-powered ECD driven by a fast-charging/discharging battery is reported. The design of this self-powered ECD is based on two primary criteria: (1) the electrochromic battery should exhibit high and continuous specific capacity, and (2) the ECD should present multiple functions for widespread use. On account of the above criteria, we selected PB as the electrochromic material and also the self-rechargeable battery component because of its ability to act as an electron reservoir.[22] Then, the electrodeposited PB film and magnesium (Mg) rod were used as cathode and anode electrodes for constructing fast-charging/recharging battery with high power-density output. The fabricated electrochromic smart windows possess several advantages, such as apparent color contrast, high reversibility, and long-time stability. More importantly, the developed self-powered ECDs can be further applied in visual detection of reactive oxygen species (ROS) with high sensitivity.

EXPERIMENTAL SECTION

Materials. KCl, $K_3[Fe(CN)_6]$, $FeCl_3{\cdot}6H_2O$, NaOH, and NaClO were purchased from Sinopharm Chemical Reagent Co., Ltd. $K_2HPO_4{\cdot}3H_2O$ and KH_2PO_4 were used to prepare the phosphate buffer. All other chemicals were of analytical grade, and ultrapure water (>18 MΩ) from a Milli-Q Plus system (Millipore) was utilized throughout the experiments. The FTO chips (transmittance > 83%, sheet resistance < 15 Ω sq^{-1}) were purchased from Zhuhai Kaivo Optoelectronic Technology Co., Ltd., China.

Apparatus. Field-emission scanning electron microscopy images were performed with an FEI Quanta200F. Absorption measurements were taken on PerkinElmer Lambda 750s. All electrochemical experiments were carried out on a CHI660 electrochemical workstation (Chenhua Instrument Corporation, China). A conventional three-electrode cell was used, including an Ag/AgCl (saturated KCl) electrode as the reference electrode, a platinum wire as the counter electrode, and the fluorine-doped tin oxide (FTO) as the working electrode. In situ spectroelectrochemical measurements were carried out in a modified luminescence cell according to a previous report at room temperature.

Preparation of PB Film. Before modification, FTO glasses of 0.80 × 5.30 cm^2 were washed with acetone, ethanol, and water sequentially, then activated in ethanol/NaOH solution under ultrasonication. Then, the FTO glasses were washed with pure water several times and dried under N_2 flow. After that, the PB films were electrodeposited under a constant potential of 0.4 V for 200, 500, and 1000 s, respectively, in an electrolyte solution of 0.1 M KCl, 0.1 M HCl, 2.5 mM $K_3[Fe(CN)_6]$, and 2.5 mM $FeCl_3$, then washed with pure water and dried at 100 °C for 5−6 h and saved in centrifuge tubes for subsequent use.

Fabrication of a Self-Powered Battery. Mg/PB battery was composed of metallic Mg and PB, which works as an anode and cathode, respectively. The part of Mg rods exposed to the air was polished each time. The electrolyte solution contains 1 M KCl, 0.1 M phosphate buffer (pH 6), and NaClO (0.0041 or 0.025 M). Through connecting and disconnecting PB and Mg electrodes, the battery can discharge and charge smoothly. Open circuit potential-time (CHI660) was used to detect the electrode potential. In addition, the performance of the Mg/PB battery was measured using chronopotentiometry with the current ramp (CHI660) method, in which PB served as the working electrode and Mg worked as both the counter and reference electrodes.

Video Record. The video of a Mg/PB battery powering a light-emitting diode (LED) for 2 h was recorded in a phosphate buffer electrolyte containing 0.025 M NaClO. The FTO slides were electrodeposited with PB under a constant potential of 0.4 V for 500 s.

RESULTS AND DISCUSSION

Electrodeposition of PB coatings onto the FTO electrode was obtained by using the chronoamperometry method under a potential of 0.4 V (Figure S1A). The typical redox peak of PB was observed in the cyclic voltammetry (CV) curves (Figure S1B), which can be ascribed to the insertion (extraction) of electrons into (out of) the PB. It is seen from the energy-level diagram that there exists a big voltage drop (about 2.4 V) between Mg (−1.8 V) and PB (0.6 V) (Figure S2), and once Mg and PB electrodes are connected, it would produce a high power-density output, making it possible to construct self-powered ECDs. Herein, the PB-film-coated FTO electrode and magnesium (Mg) rod were used as the cathode and anode of the battery, and at the same time, the PB film worked as the electrochromic layer.

The bleaching process of the EC device corresponds to the discharge process of the battery, whereas the coloring process corresponds to the charge process. Therefore, the amount of charge during the charge−discharge tests was first conducted, which can deliver the same capacity under current densities of 0.1, 0.2, 0.5, 1.0, and 2.0 A m^{-2} (Figure 1A). When cycled at a current density of 0.5 A m^{-2}, a capacity of 21.5 mA h m^{-2} is obtained in the first cycle and it still can deliver a discharge capacity of 20.2 mA h m^{-2} after three cycles (Figures 1B and S3). Figure 1C reveals the high cycling stability of the battery. Compared with the first discharge process, nearly 80% of the

DOI: 10.1021/acsami.9b08715
ACS Appl. Mater. Interfaces XXXX, XXX, XXX−XXX

initial capacity are retained after 20 cycles, indicating a better performance than previous electrochromic batteries.

Figure 2A shows the in situ absorbance measurement of the fabricated two-electrode battery. The switching time is a direct

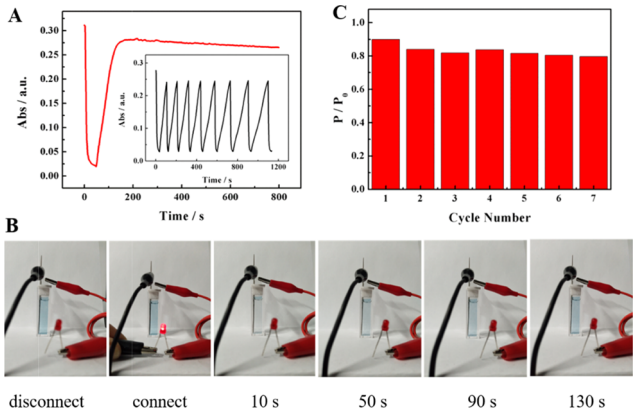

Figure 2. (A) In situ absorbance (located at 698 nm) measurement of the prepared battery (connection for 50 s and cut off), and the repeated charging and discharging cycles with PB and Mg electrodes (connection for 30 s and disconnection at different times, inset) and (B) the corresponding photographs of the two electrodes (from left to right) open, connecting for 8 s, and disconnecting for 10, 50, 90, and 130 s, respectively. (C) Cyclic recharging of the Mg/PB battery in an electrolyte containing 4 mM NaClO. The PB films are electrodeposited under a constant potential of 0.4 V for 200 s.

kinetics parameter for the electrochromic process. The absorbance intensity abruptly decreased from 0.3 to 0.02 after the two-electrode connection for 50 s. The contrast ratio of the film between the steady colored and bleached states is about 0.9. Then, by cutting the connection, the absorbance would recover to be about 0.27 in 50 s and it can maintain 95% of the original value after the 10 min test. Furthermore, the switching is well reversible between the "on" and "off" states and there are no noticeable absorbance changes after several cycles (inset of Figure 2A). Compared with most reported self-powered ECDs, this system displays a quick response. The coloration time and bleaching time are 20 and 80 s in the first operation, respectively. Accompanied by the NaClO consumption, the recovery process became slightly slow, but still can reach the original absorbance value in 200 s in the final cycle. In addition, the bleaching and recovering process was recorded in detail (Figure 2B). First, PB existed in the original oxidative state, at which PB presented strong UV absorption with blue PB with an Mg electrode; then, PB was reduced to Prussian white (PW) accompanied by intervalence charge transfer elimination from Fe(III) to Fe(II), and the corresponding blue color becomes transparent with weak absorption (Figure S4). Then, by cutting off the connection of the two electrodes, the system could gradually recover from the reduced state to its original state again by the oxidation of NaClO. It is remarkable that this process presents battery characteristics. Therefore, we characterized the rechargeable ability of Mg/PB ECDs, which delivered a power density of about 4 mW cm^{-2} in the first discharging process, and about 90% of the maximum power density could be retained after seven cycles (Figure 2C). After 20 cycles, the capacity of the electrochromic battery declined about 20%, which suggested relative cycling stability of the fabricated self-powered device (Figure S6). Moreover, this smart ECD shows vast potential applications in electrochromic windows. For example, the color of the electrochromic bedroom's windows can be adjusted to protect the user's privacy.[5] The colored degree of the window depended on the thickness of the PB coating, which can be well controlled by the deposition time. As shown in Figure 3,

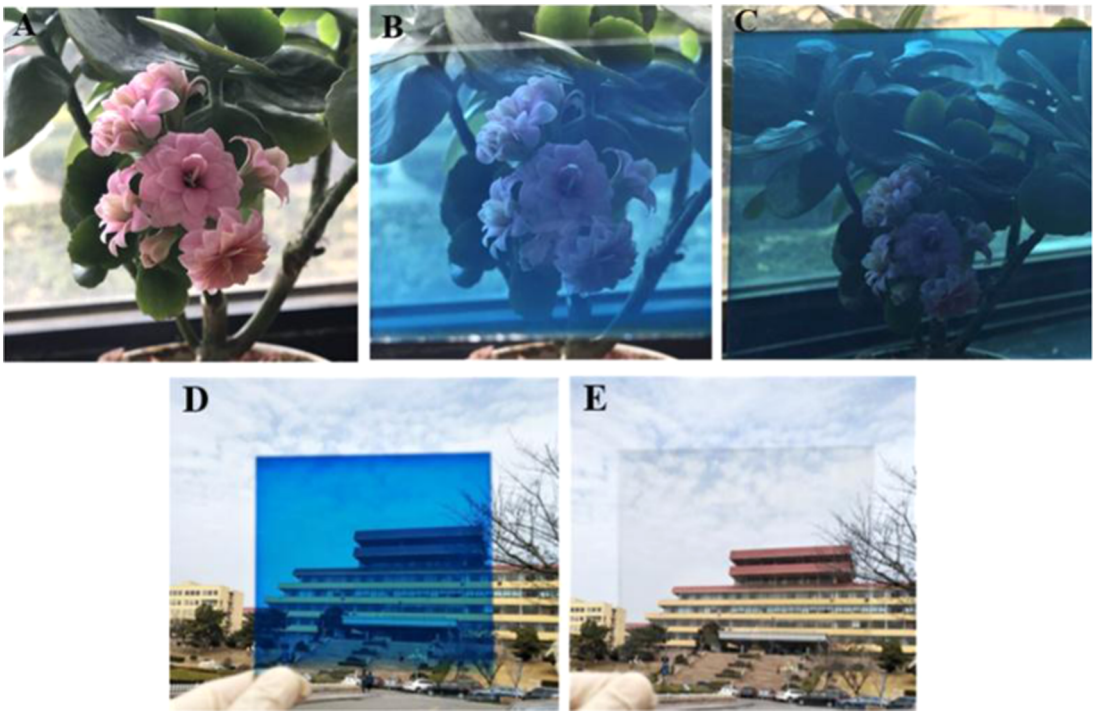

Figure 3. Digital photograph of object (A), covered with colored ECDs (B–D) and bleached ECDs (E). The PB films electrodeposited under a constant potential of 0.4 V for 500 s (B) and 1000 s (C–E) were used for cathode electrodes.

DOI: 10.1021/acsami.9b08715
ACS Appl. Mater. Interfaces XXXX, XXX, XXX–XXX

the flower is blurry through FTO deposited with PB for 500 s (B), whereas the flower and building are invisible through FTO with a 1000 s PB film (C, D). Once PB is connected with Mg, the electrochromic film bleached and the background became transparent (E).

Self-powered electrochromic sensors are analytical devices generating their own energy without any external stimulus. The first example of self-powered ECDs used for biosensors was proposed by Willner et al., which was powered by biofuel cells, but it is hard to give quantitative information of analyte concentration.[23] Herein, in conjunction with electrochromic windows, the self-powered ECD can also be utilized as an ROS sensor. It is especially noteworthy that proteins, nucleic acids, and lipids can be directly oxidized by highly strong ROS (hROS) including •OH, ClO^-, $ONOO^-$, etc., which play a central role in many human pathologies.[24,25] Despite its importance, there is still a lack of sensitive methods for hROS detection. In this work, NaClO was employed as a model molecule to monitor the concentration change of ROS in real time. The cathode turns to be PW after discharge by connecting with Mg and would be reoxidized to be PB in the presence of NaClO.[26] Figure 4A shows the direct

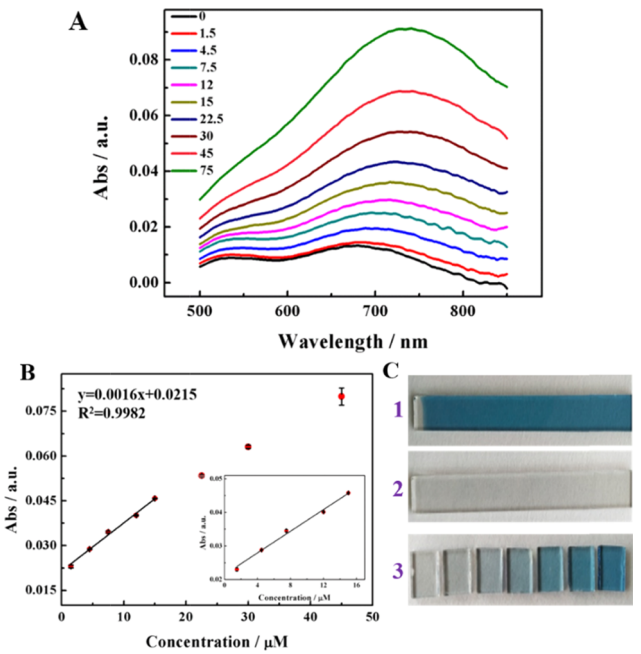

Figure 4. (A) Absorbance response of PW with the addition of different NaClO concentrations (0, 1.5, 4.5, 7.5, 12, 15, 22.5, 30, 45, and 75 μM). (B) The peak height of the absorbance at 698 nm as a function of NaClO concentration (R^2 = 0.9982). (C) The photograph of PB, first connection with Mg and turned to be colorless PW, then gradually recovered to be PB with different amounts of NaClO (from left to right: 1.5, 2.25, 3, 3.75, 4.5, and 5.6 mM)

transmittance variation of the PW in response to the different NaClO concentrations. Due to the low background signal of the "turn-on" sensor, this method has a good linear relationship with the concentration of NaClO ranging from 1.5 to 15 μM, with a low detection limit of 0.22 μM (Figure 4B). It is worth noting that the results are better than those obtained by dual-emission fluorescent[27] and bioluminogenic probes[24] and electrocatalytic[28] methods. The mechanism could be illustrated as follows: the oxidation potential of NaClO is much higher than PW, indicating that a small amount of NaClO could achieve the oxidation of PW to PB, and then the lower detection limit of NaClO is obtained.

$$K_2Fe^{2+}[Fe^{2+}(CN)_6]\ (PW) - e^- = KFe^{3+}[Fe^{2+}(CN)_6]\ (PB) + K^+ - 0.43\ V\ (vsSHE) \quad (1)$$

$$HClO + H^+ + 2e^- = Cl^- + H_2O + 1.482\ V\ (vsSHE) \quad (2)$$

Interestingly, the as-fabricated ECDs can be used for the visual detection of ROS, and the bleaching and recovering process is recorded in Figure 4C. Notably, after connection with Mg, PB-based ECDs with blue color turned to white (PW). After addition of different concentrations of NaClO, PW was gradually oxidized to PB by NaClO, and the color of the PW film changed to initial blue again, which reveals that this ECD can be used for ROS sensitive and visual detection.

To demonstrate the concept of multifunctional ECDs, a new strategy was proposed by integrating self-rechargeable battery and powering electronic devices into one device. Interestingly, the as-fabricated ECDs are proven to show excellent energy-storage properties. It was bleached totally with an optical transmittance of about 91.3% after connecting with Mg for 1 min and delivered a high specific capacitance of about 5.7 mW cm^{-2} (Figure 5A). For continuous and stable energy supply applications, two factors should be balanced: one is high power density and the other is stable output. If the battery discharged completely one-time, it cannot supply continuous power source. It has been proven that oxidants such as NaClO, H_2O_2, and $(NH_4)_2S_2O_8$ can effectively improve the output power of the fabricated system. But the concentration of oxidants needs to be optimized strictly. On the one hand, NaClO should accelerate the charging of the battery effectively, but the concentration cannot be high, otherwise the Mg will be oxidized seriously. Taking the two factors into account, we tried a series of NaClO concentrations such as 8, 12, 25, and 30 mM, and finally the concentration of NaClO was optimized to be 0.025 M. As shown in Figure 5B, by connecting the two electrodes, the absorption intensity of the PB film decreased from 0.5 to 0.26. Because of the strong oxidation of NaClO, about 50% amount of PB cannot be reduced to PW, and the absorption intensity maintained at about 0.33. A video recording of the in situ color changes during 2 h connection is presented (Figure S5), which shows that the film can steadily maintain this middle state without noticeable loss. Furthermore, the delivered energy can continuously light up a light-emitting diode (LED) for more than 2 h, which demonstrates the smart ECD to possess excellent energy-storage properties. In addition, the surface morphology of PB before and after cycling was studied. As shown in Figure S6, after the 2 h test, the morphology of the PB film remained unchanged except a more compact structure with larger globules, and the blue film turned to light blue. Therefore, the proposed smart glass windows show great potential in powering electronic devices.

CONCLUSIONS

In summary, we have proposed a strategy to design multifunctional self-powered electrochromic displays driven by Mg/PB battery, which can be self-charged and recharged within 50 s. Compared with traditional electricity-triggered ECDs, the as-developed self-powered ECDs present several

DOI: 10.1021/acsami.9b08715
ACS Appl. Mater. Interfaces XXXX, XXX, XXX−XXX

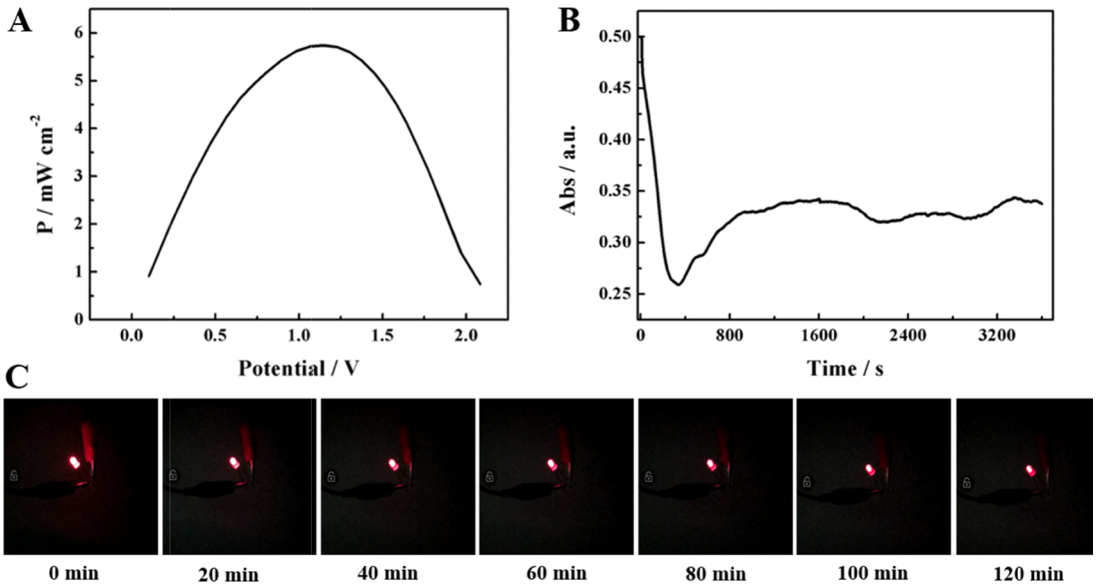

Figure 5. (A) Dependence of the power density on the cell voltage of the self-powered battery. The anode was an electrodeposited PB film under a constant potential of 0.4 V for 500 s with 0.025 M NaClO. (B) In situ absorbance (698 nm) measurement of the Mg/PB battery for 2 h connection in PBS with 0.025 M NaClO. (C) The corresponding photographs of the curves refer to the two electrodes connecting for 0, 20, 40, 60, 80, 100, and 120 min. The images were extracted from the video taken during the capacitive process.

advantages such as facile operation, apparent absorbance contrast, large reversibility, and stability. Moreover, these ECDs exhibit promising application in electrochromic windows to balance the indoor light. In addition, self-powered ECDs can also be utilized for highly sensitive ROS sensing and visual analysis. More importantly, as-prepared ECDs are proven to show excellent energy-storage properties with high output voltage for continuous and stable energy supply. Above all, these multifunctional self-powered ECDs are important not only for exhibiting promising applications in self-powered smart window and ROS sensor fields but also for providing a solution for energy supply problems.

■ ASSOCIATED CONTENT

Supporting Information

The Supporting Information is available free of charge on the ACS Publications website at DOI: 10.1021/acsami.9b08715.

i–*t* curve obtained during PB formation; CV curve of PB; diagram of the energy level of PB and Mg for electrochromic battery; charge–discharge profiles of the battery at a current density of 0.5 A m^{-2} in the potential range of 0–0.35 V; photographs of the prepared PB/Mg battery in colored and bleached states, and corresponding absorbance spectra; photograph and TEM image of the PB film before and after the 2 h test (PDF)

Lit-up LED powered by the fabricated ECD for 2 h at a 16× play speed (MP4)

■ AUTHOR INFORMATION

Corresponding Authors

*E-mail: zhaiyanling@qdu.edu.cn (Y.Z.).
*E-mail: zhuzhujun001@gmail.com (Z.Z.).
*E-mail: dongsj@ciac.ac.cn (S.D.).

ORCID

Zhijun Zhu: 0000-0001-6376-5041
Shaojun Dong: 0000-0003-3197-7204

Notes

The authors declare no competing financial interest.

■ ACKNOWLEDGMENTS

This work was supported by the National Natural Science Foundation of China (21804074), the Natural Scientific Foundation of Shandong Province (ZR2018BB051), and the Open Funds of the State Key Laboratory of Electroanalytical Chemistry (SKLEAC201906).

■ REFERENCES

(1) Granqvist, C. G. Electrochromic devices. *J. Eur. Ceram. Soc.* **2005**, *25*, 2907–2912.
(2) Zhai, Y.; Zhu, Z.; Zhou, S.; Zhu, C.; Dong, S. Recent advances in spectroelectrochemistry. *Nanoscale* **2018**, *10*, 3089–3111.
(3) Zhou, Y.; Fang, J.; Wang, H. X.; Zhou, H.; Yan, G. L.; Zhao, Y.; Dai, L. M.; Lin, T. Multicolor Electrochromic Fibers with Helix-Patterned Electrodes. *Adv. Electron. Mater.* **2018**, *4*, No. 1800104.
(4) Nielsen, C. B.; Angerhofer, A.; Abboud, K. A.; Reynolds, J. R. Discrete photopatternable pi-conjugated oligomers for electrochromic devices. *J. Am. Chem. Soc.* **2008**, *130*, 9734–9746.
(5) Gu, H.; Guo, C.; Zhang, S.; Bi, L.; Li, T.; Sun, T.; Liu, S. Highly Efficient, Near-Infrared and Visible Light Modulated Electrochromic Devices Based on Polyoxometalates and W18O49 Nanowires. *ACS Nano* **2018**, *12*, 559–567.
(6) Zheng, R.; Wang, Y.; Jia, C. Y.; Wan, Z. Q.; Luo, J. S.; Malik, H. A.; Weng, X. L.; Xie, J. L.; Deng, L. J. Intelligent Biomimetic Chameleon Skin with Excellent Self-Healing and Electrochromic Properties. *ACS Appl. Mater. Interfaces* **2018**, *10*, 35533–35538.
(7) Yang, P.; Sun, P.; Mai, W. Electrochromic energy storage devices. *Mater. Today* **2016**, *19*, 394–402.
(8) Thompson, B. C.; Kim, Y. G.; McCarley, T. D.; Reynolds, J. R. Soluble narrow band gap and blue propylenedioxythiophene-cyanovinylene polymers as multifunctional materials for photovoltaic and electrochromic applications. *J. Am. Chem. Soc.* **2006**, *128*, 12714–12725.
(9) Zhai, Y.; Jin, L.; Zhu, C.; Hu, P.; Han, L.; Wang, E.; Dong, S. Reversible electroswitchable luminescence in thin films of organic-inorganic hybrid assemblies. *Nanoscale* **2012**, *4*, 7676–7681.

(10) Yang, X.; Zhu, G.; Wang, S.; Zhang, R.; Lin, L.; Wu, W.; Wang, Z. L. A self-powered electrochromic device driven by a nanogenerator. *Energy Environ. Sci.* **2012**, *5*, 9462−9466.
(11) Gu, H.; Bi, L.; Fu, Y.; Wang, N.; Liu, S.; Tang, Z. Multistate electrically controlled photoluminescence switching. *Chem. Sci.* **2013**, *4*, 4371−4377.
(12) Zhai, Y.; Zhu, Z.; Zhu, C.; Zhu, J.; Ren, J.; Wang, E.; Dong, S. Reversible photo-chem-electrotriggered three-state luminescence switching based on core-shell nanostructures. *Nanoscale* **2013**, *5*, 4344−4350.
(13) Zhu, M.; Huang, Y.; Ng, W. S.; Liu, J.; Wang, Z.; Wang, Z.; Hu, H.; Zhi, C. 3D spacer fabric based multifunctional triboelectric nanogenerator with great feasibility for mechanized large-scale production. *Nano Energy* **2016**, *27*, 439−446.
(14) Xie, Z.; Jin, X.; Chen, G.; Xu, J.; Chen, D.; Shen, G. Integrated smart electrochromic windows for energy saving and storage applications. *Chem. Commun.* **2014**, *50*, 608−610.
(15) Dyer, A. L.; Bulloch, R. H.; Zhou, Y.; Kippelen, B.; Reynolds, J. R.; Zhang, F. A Vertically Integrated Solar-Powered Electrochromic Window for Energy Efficient Buildings. *Adv. Mater.* **2014**, *26*, 4895−4900.
(16) Bai, L.; Jin, L.; Han, L.; Dong, S. Self-powered fluorescence controlled switch systems based on biofuel cells. *Energy Environ. Sci.* **2013**, *6*, 3015−3021.
(17) Wu, X.; Zheng, J.; Xu, C. A newly-designed self-powered electrochromic window. *Sci. China Chem.* **2017**, *60*, 84−89.
(18) Pu, X.; Li, L.; Liu, M.; Jiang, C.; Du, C.; Zhao, Z.; Hu, W.; Wang, Z. L. Wearable Self-Charging Power Textile Based on Flexible Yarn Supercapacitors and Fabric Nanogenerators. *Adv. Mater.* **2016**, *28*, 98−105.
(19) Zhang, H.; Yu, Y.; Zhang, L.; Zhai, Y.; Dong, S. Self-powered fluorescence display devices based on a fast self-charging/recharging battery (Mg/Prussian blue). *Chem. Sci.* **2016**, *7*, 6721−6727.
(20) Wang, J.; Zhang, L.; Yu, L.; Jiao, Z.; Xie, H.; Lou, X. W.; Wei Sun, X. A bi-functional device for self-powered electrochromic window and self-rechargeable transparent battery applications. *Nat. Commun.* **2014**, *5*, No. 4921.
(21) Yang, B.; Ma, D.; Zheng, E.; Wang, J. A self-rechargeable electrochromic battery based on electrodeposited polypyrrole film. *Sol. Energy Mater. Sol. Cells* **2019**, *192*, 1−7.
(22) Nossol, E.; Zarbin, A. J. G. A Simple and Innovative Route to Prepare a Novel Carbon Nanotube/Prussian Blue Electrode and its Utilization as a Highly Sensitive H_2O_2 Amperometric Sensor. *Adv. Funct. Mater.* **2009**, *19*, 3980−3986.
(23) Katz, E.; Bückmann, A. F.; Willner, I. Self-Powered Enzyme-Based Biosensors. *J. Am. Chem. Soc.* **2001**, *123*, 10752−10753.
(24) Kojima, R.; Takakura, H.; Kamiya, M.; Kobayashi, E.; Komatsu, T.; Ueno, T.; Terai, T.; Hanaoka, K.; Nagano, T.; Urano, Y. Development of a Sensitive Bioluminogenic Probe for Imaging Highly Reactive Oxygen Species in Living Rats. *Angew. Chem., Int. Ed.* **2015**, *54*, 14768−14771.
(25) Zhai, Y.; Zhu, C.; Ren, J.; Wang, E.; Dong, S. Multifunctional polyoxometalates-modified upconversion nanoparticles: integration of electrochromic devices and antioxidants detection. *Chem. Commun.* **2013**, *49*, 2400−2402.
(26) Zloczewska, A.; Celebanska, A.; Szot, K.; Tomaszewska, D.; Opallo, M.; Jönsson-Niedziolka, M. Self-powered biosensor for ascorbic acid with a Prussian blue electrochromic display. *Biosens. Bioelectron.* **2014**, *54*, 455−461.
(27) Chen, T.; Hu, Y. H.; Cen, Y.; Chu, X.; Lu, Y. A Dual-Emission Fluorescent Nanocomplex of Gold-Cluster-Decorated Silica Particles for Live Cell Imaging of Highly Reactive Oxygen Species. *J. Am. Chem. Soc.* **2013**, *135*, 11595−11602.
(28) Rawson, F. J.; Hicks, J.; Dodd, N.; Abate, W.; Garrett, D. J.; Yip, N.; Fejer, G.; Downard, A. J.; Baronian, K. H. R.; Jackson, S. K.; Mendes, P. M. Fast, Ultrasensitive Detection of Reactive Oxygen Species Using a Carbon Nanotube Based-Electrocatalytic Intracellular Sensor. *ACS Appl. Mater. Interfaces* **2015**, *7*, 23527−23537.

DOI: 10.1021/acsami.9b08715
ACS Appl. Mater. Interfaces XXXX, XXX, XXX−XXX